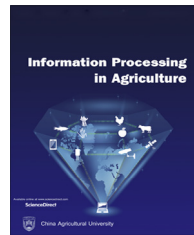




Available at www.sciencedirect.com

INFORMATION PROCESSING IN AGRICULTURE 7 (2020) 58–71

journal homepage: www.elsevier.com/locate/inpa



Design and simulation of an integrated end-effector for picking kiwifruit by robot



Longtao Mu ^a, Gongpei Cui ^a, Yadong Liu ^b, Yongjie Cui ^{a,c,d,*}, Longsheng Fu ^{a,c,d}, Yoshinori Gejima ^e

^a College of Mechanical and Electronic Engineering, Northwest A&F University, Yangling, Shaanxi 712100, China

^b China Aviation Lithium Battery Research Institute Co., Ltd, Changzhou, Jiangsu 213200, China

^c Key Laboratory of Agricultural Internet of Things, Ministry of Agriculture and Rural Affairs, Yangling, Shaanxi 712100, China

^d Shaanxi Key Laboratory of Agricultural Information Perception and Intelligent Service, Yangling, Shaanxi 712100, China

^e Faculty of Agriculture, University of Miyazaki, Miyazaki 8892192, Japan

ARTICLE INFO

Article history:

Received 30 November 2018

Received in revised form

16 April 2019

Accepted 22 May 2019

Available online 29 May 2019

ABSTRACT

The harvesting of fresh kiwifruit is a labor-intensive operation that accounts for more than 25% of annual production costs. Mechanized harvesting technologies are thus being developed to reduce labor requirements for harvesting kiwifruit. To improve the efficiency of a harvesting robot for picking kiwifruit, we designed an end-effector, which we report herein along with the results of tests to verify its operation. By using the established method of automated picking discussed in the literature and which is based on the characteristics of kiwifruit, we propose an automated method to pick kiwifruit that consists of separating the fruit from its stem on the tree. This method is experimentally verified by using it to pick clustered kiwifruit in a scaffolding canopy cultivation. In the experiment, the end-effector approaches a fruit from below and then envelops and grabs it with two bionic fingers. The fingers are then bent to separate the fruit from its stem. The grabbing, picking, and unloading processes are integrated, with automated picking and unloading performed using a connecting rod linkage following a trajectory model. The trajectory was analyzed and validated by using a simulation implemented in the software Automatic Dynamic Analysis of Mechanical Systems (ADAMS). In addition, a prototype of an end-effector was constructed, and its bionic fingers were equipped with fiber sensors to detect the best position for grabbing the kiwifruit and pressure sensors to ensure that the damage threshold was respected while picking. Tolerances for size and shape were incorporated by following a trajectory groove from grabbing and picking to unloading. The end-effector separates clustered kiwifruit and automatically grabs individual fruits. It takes on average 4–5 s to pick a single fruit, with a successful picking rate of 94.2% in an orchard test featuring 240 samples. This study shows the grabbing–picking–unloading robotic end-effector has significant potential to facilitate the harvesting of kiwifruit.

© 2019 China Agricultural University. Production and hosting by Elsevier B.V. on behalf of KeAi. This is an open access article under the CC BY-NC-ND license (<http://creativecommons.org/licenses/by-nc-nd/4.0/>).

* Correspondence author at: College of Mechanical and Electronic Engineering, Northwest A&F University, Xinong Road, 22, Yangling, 712100 Shaanxi, China.

E-mail address: cuiyongjie@nwsuaf.edu.cn (Y. Cui).

Peer review under responsibility of China Agricultural University.

<https://doi.org/10.1016/j.inpa.2019.05.004>

2214-3173 © 2019 China Agricultural University. Production and hosting by Elsevier B.V. on behalf of KeAi.

This is an open access article under the CC BY-NC-ND license (<http://creativecommons.org/licenses/by-nc-nd/4.0/>).

1. Introduction

China is the largest producer of kiwifruit (*Actinidia deliciosa*), with 56% of the world's output. Its annual output was approximately 2.39 million metric tons in 2016 from a cultivated area of over 67 000 ha [1]. The harvesting of kiwifruit is a labor-intensive operation that accounts for over 25% of annual production costs [2]. Therefore, to reduce the labor requirements, mechanized harvesting technologies are being developed and, in this context, research on harvesting robots is essential. However, the complex environment in which kiwifruit are grown and the ease with which their peel can be damaged make it difficult for robots to automatically pick kiwifruit [3]. Robotic harvesting still needs to overcome many challenges before it can be commercially viable. There are three main aspects of harvesting: approaching a target kiwifruit while avoiding obstacles [4], non-destructive separation of the fruit from the tree [5], and building a mechanical structure adapted to the farm environment and to the characteristics of the fruit [6]. Economical, efficient, and adaptable robots are thus needed to reduce the labor requirement for harvesting kiwifruit.

According to a survey by Bac et al., 50 harvesting robots have been developed over the past 30 years. For some of these robots, almost all end-effectors were custom made [6]. The end-effectors play a key role in automated fruit harvesting, and therefore their design is particularly important [5,7,8]. For other fruits and vegetables, end-effectors have been developed that make use of the ability of robots to recognize the environmental differences associated with different crops, such as tomatoes [9–11], cucumbers [12,13], apples [14–17], strawberries [18], peppers [19,20], and cherry tomatoes [20,21]. Different fruits and vegetables have different characteristic growth patterns, so the corresponding harvesting methods that use end-effectors also differ [5,22]. These end-effectors harvest fruits in three steps. First, they grasp or suck the fruit. Second, they detach the fruit by rotating, pulling, or cutting it using tools such as scissors, lasers, or water knives. Third, they unload the fruit into a collection box and reset the end-effector. Most end-effectors require three proximity processes to harvest the fruit: grabbing, picking, and unloading. The related problems include complex control procedures, cumulative errors, and a low success rate of harvesting.

In contrast with apples [15,23,24], citrus fruits [25–27], and some fruits grown on separate trees, grapes [28] and kiwifruit are grown using scaffolding cultivation, bushes, or vines in a relatively standardized growth environment. This type of cultivation requires a large ground area without obstacles so that it is suitable for mechanized picking [29]. Furthermore, based on artificial picking, the bending and picking method are similar to manual picking because of the small detachment force, short travel distance, and high efficiency [5]. The kiwi peel can be easily damaged [30] so the clamping force should be minimized during picking. The clamping force should consider the degree of ripening, clustering, and other characteristics. Although several studies have focused on robotic end-effectors for harvesting kiwifruit [5,22,31–33], they did not

completely integrate the grabbing-picking-unloading operations. Thus, the purpose of the present study is to design and test an efficient and flexible end-effector that overcomes the challenges posed by the ease of damage to the peel, slow picking without unloading, and the complex mechanisms involved.

For this work, we considered the Hayward variety of kiwifruit and developed an end-effector suitable for picking fruit in an orchard. We propose a simple reciprocating motion using an end-effector to implement the complex motion involved in the grasping, picking, and unloading of fruit. We first theoretically analyzed an integrated linkage method with a trajectory model slot of an anti-cam mechanism that quickly implements the complex movement of a round trip grasping-picking-unloading motion. Next, we analyzed and validated the trajectory by using a simulation implemented in the software Automatic Dynamic Analysis of Mechanical Systems (ADAMS). The correctness and feasibility of the theoretical trajectory of a prototype end-effector were verified by comparison with the simulated trajectory. Finally, a custom-made end-effector was assembled on an experimental platform of a kiwifruit-picking robot and subjected to field tests. The results demonstrate that the kiwifruit harvesting robot can pick fruit with a reasonable success rate, which means that the proposed end-effector is commercially viable.

In Section 2, we survey the crop environment, end-effector, and hardware and software. Section 3 outlines our experiment and gives the results, and Section 4 discusses various aspects of operating an end-effector in an orchard. Finally, Section 5 presents the main conclusions of this work.

2. Material and methods

2.1. Parameters of kiwifruit cultivation

For Hayward kiwifruit grown at the Meixian Kiwifruit Experimental Station of the Northwest Agriculture and Forestry University (34°07'39" N, 107°59'50" E, 648 m altitude), published data and sample statistics give the following physical parameters. The scaffolding for the kiwifruit cultivation is mainly built from steel pipes and iron wire. Two fruit trees were planted between two vertical steel columns, each 1.80 m high and separated by 4 m. Fig. 1(a) shows the trees and the scaffolding, and Fig. 1(b) shows a cluster of kiwifruit on a tree.

The physical and geometrical properties of kiwifruit include its shape, size, friction coefficient, and separation force. In October 2015 and 2016, 120 Hayward kiwifruit were randomly selected for measurement from a total of 300. The size and mass were measured using electronic Vernier calipers and electronic scales (accuracy 0.1 g). Friction was measured using an inclined rubber plate and a universal micro-control electronic testing machine (HY0230; Shanghai Hengyi Precision Instrument Co., Ltd.; see Fig. 2), which has an accuracy of 0.3% from 1 to 2000 N.

The static friction coefficient between kiwifruit and the rubber was determined as follows: Five or six kiwifruit were tightly packed in a single row in a bottomless box (175 mm

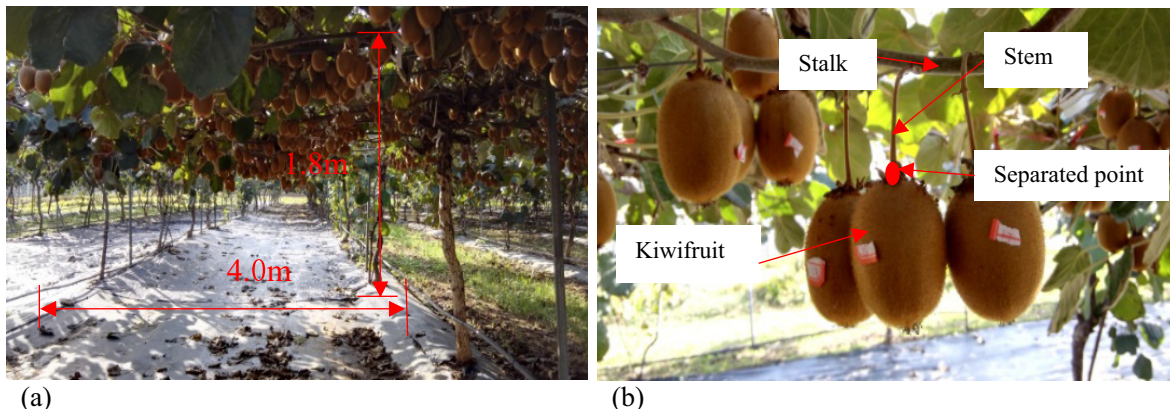


Fig. 1 – (a) Kiwifruit cultivation using scaffolding. (b) Photograph of kiwifruit attached by its stem to the stalk of a tree.



Fig. 2 – Friction-measuring device. Shown are the bottomless box, HY0230 testing machine, and rubber plate. The angle θ is between the inclined plane and the horizontal.

long, 115 mm wide, 40 mm high). The surface of the kiwifruit was placed in contact with the horizontal rubber plate. The HY0230 lifted the edge of the rubber plate at a speed of 90 mm/min, as shown in Fig. 2. The inclination angle θ of the rubber plate was recorded at the point where the kiwifruit and the box began to slide, and the static friction coefficient was calculated from this angle. Each of the 10 groups of fruit was tested three times.

The force needed to separate a fruit from its stem was measured experimentally by using the 120 Hayward kiwifruit mentioned above, randomly divided into six groups. The samples were picked on the same day in 2016. The apparatus is shown in Fig. 3. The fruit was held at different angles on the base of the HY0230 testing machine by clamp 2, and the fruit stem was held on the movable beam of the machine by clamp 1. For each group, the force was measured at one of five angles: 90°, 75°, 60°, 45°, and 30°. The picking angle between the long axis of the fruit and the stem was set by using a protractor [5]. The HY0230 testing machine then applied a force to the stem. The testing machine automatically recorded

the separation force when the fruit stem detached from the fruit, and the average separation force for each group was calculated.

The force required to separate the kiwifruit from its stem equals the two-finger force of the end-effector when holding a kiwifruit. The negative force in the axial direction of the kiwifruit is given by the static friction coefficient multiplied by the two-finger force. Therefore, the kiwifruit separation force F_s is

$$F_s = 2F_f, \quad (1)$$

where $F_f = \mu F$ is the static friction force (N), μ is the static friction coefficient, and F is the two-finger pressure force (N).

The average physical parameters of the fruits were as follows: width = 52.16 mm, thickness = 47.86 mm, length = 64.98 mm, stalk length = 58.7 mm, rubber friction coefficient ranged from 0.38 to 0.51, maximum friction angle = 27°. Table 1 lists the main physical parameters of the kiwifruit as measured in the laboratory. The shape and size were the main parameters used for designing the end-effector, whereas the separation force was required for designing the control system.

Fig. 4 illustrates the pull-down method for picking kiwifruit. The force required to separate a kiwifruit from its stem is minimal when the long axis of the fruit and the peduncle of the stem form a 60° angle. The point B is where the stalk joins the fruit. The fingers of the end-effector grasp the fruit at point B, and the fruit is separated from the stalk at point B''. At the instant of fruit separation, the finger of the end-effector, fruit, and stalk form a hinge (where point C is the end-effector's hinge joint), following which the fingers continue to move and open. Finally, the end-effector mechanism pulls down on the fruit. The picked fruit then slides down into a collection basket protected by a soft buffer material. This pull-down picking method differs from that described by Fu et al. [5], in which the fruit were bent upward.

2.2. Inverse cam mechanism

The simplified inverse cam mechanism is shown in Fig. 5(a). The cam consists of a rolling bearing at a pendulum angle of 60° to minimize the movement of the rod. The displacement s (m) of the inverse cam mechanism is given as

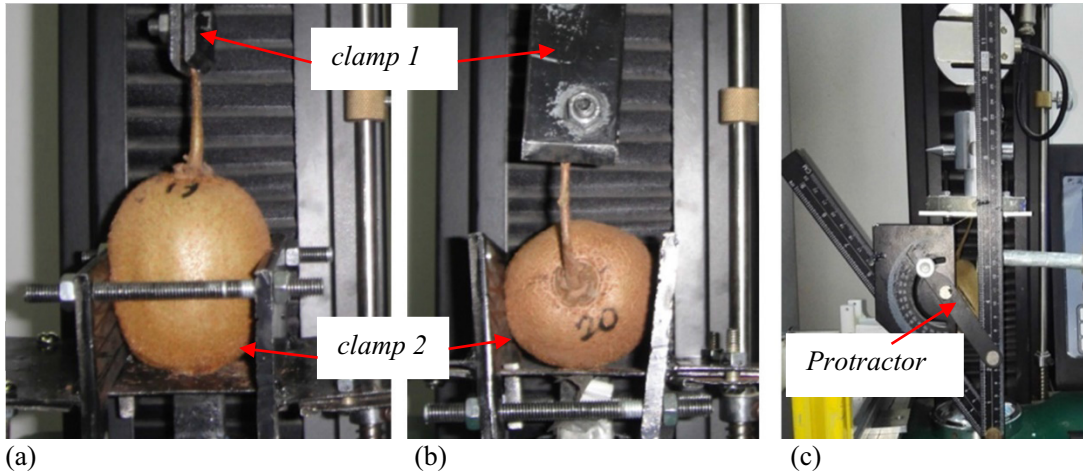


Fig. 3 – Detachment test of stem and definition of angle. The angle during the picking test was measured between the inertial axis of the fruit stem and the kiwifruit [5].

Table 1 – Physical parameters of Hayward kiwifruit in China.

	Weight (g)	Minor axis (mm)	Major axis (mm)	Separation force (N)	Static friction coefficient	Curvature
Average	97.40	47.86	52.26	4.91	0.44	32.50
Range	81.40–128.70	42.70–51.84	45.85–57.13	1.08–12.25	0.38–0.51	28.50–35.30
Error	±0.15	±0.35	±0.43	±0.51	±0.05	±0.16

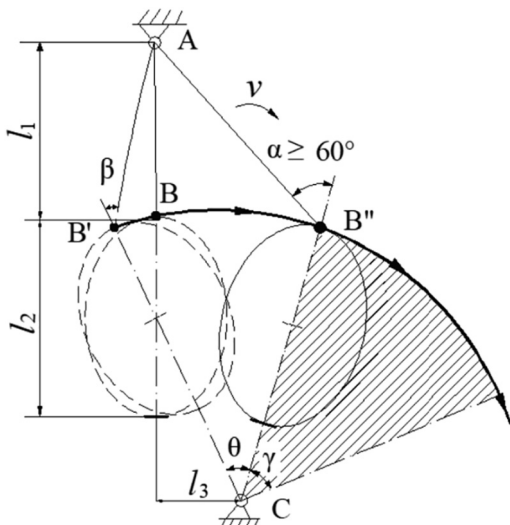


Fig. 4 – Geometry of picking method. Point A is the link between the tree and the stem, point B is the link between the kiwifruit and the stem, and l_1 is the stem distance. Point C is the end-effector's hinge joint. The kiwifruit is moved to position B'' , and the stem and the kiwifruit separate. $B'B$ is the grasped part of the end-effector's trajectory and BB'' is the picked part of its trajectory. From point B'' is the unloading part of the end-effector's trajectory.

$$s = C_0 + C_1\delta^1 + C_2\delta^2 + \dots + C_n\delta^n, \quad (2)$$

where C_n are undetermined coefficients and δ is the angle of rotation of the cam ($^\circ$). The boundary conditions are $\delta = 0$,

$s = 0$ at the start point and $\delta = 0$, $s = h$ at the stop point. If $C_0 = 0$, then $C_1 = h/\delta_0$. The forward motion of the push rod is given by

$$\begin{aligned} s &= \frac{h\delta}{\delta_0}, \\ v &= \frac{h\omega}{\delta_0}, \\ \alpha &= 0, \end{aligned} \quad (3)$$

where h is the distance traveled (m), δ_0 is the angle of the cam ($^\circ$), v is the velocity of motion ($m s^{-1}$), ω is the angular velocity (rad), and α is angular acceleration ($m s^{-2}$).

During the return phase, the motion of the rod can be described by

$$\begin{aligned} s &= h\left(1 - \frac{\delta}{\delta_0}\right), \\ v &= -\frac{h\omega}{\delta_0}, \\ \alpha &= 0, \end{aligned} \quad (4)$$

where δ' is the return angle of the cam ($^\circ$).

The velocity of the push rod is

$$\begin{aligned} v &= v_p = \overline{OP}\omega, \\ \overline{OP} &= \frac{v}{\omega} = \frac{ds}{d\delta}, \end{aligned} \quad (5)$$

where P is the instantaneous center between cam and rod.

The coordinates of the profile position B of the cam are given by

$$\begin{aligned} x &= (r_0 + s)\sin\delta + \left(\frac{ds}{d\delta}\right)\cos\delta, \\ y &= (r_0 + s)\cos\delta - \left(\frac{ds}{d\delta}\right)\sin\delta, \end{aligned} \quad (6)$$

where r_0 is the radius of the base circle of the cam (m).

Thus, when $O = 60^\circ$, $x = 31.18$ mm, and $y = 36$ mm, the track groove movement is 18 mm. The trajectory from the ini-

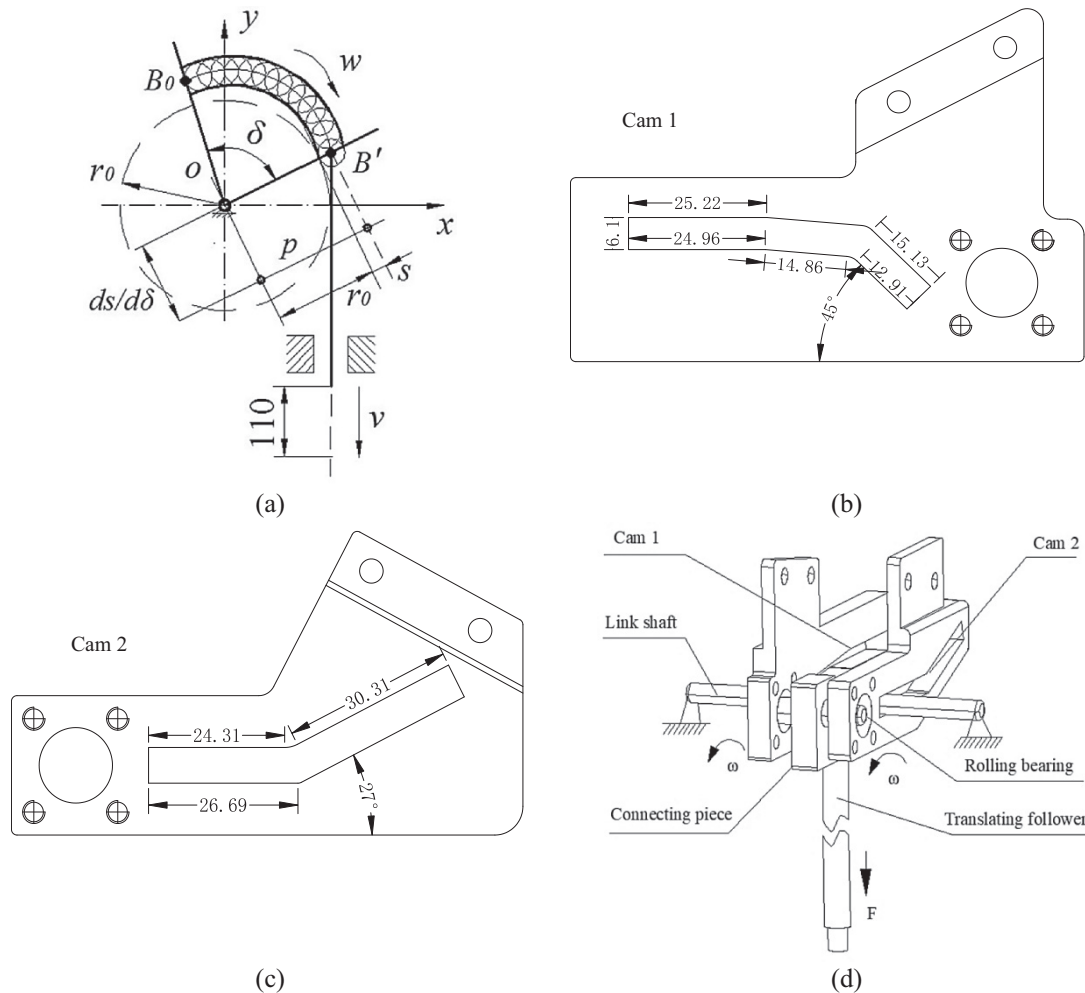


Fig. 5 – (a) Inverse cam mechanism. (b), (c) Schematic of integrated inverse guidance cam. (d) Rolling bearing with a pendulum angle to minimize rod movement.

tial grab and tight grasping to the parting of the fingers and unloading of the fruit by the end-effector was designed based on these parameters, as shown in Fig. 5(b)–(d).

2.3. Simulation of structural kinetics

The trajectory of finger movement was determined according to the trajectory of the centroid of the fruit to allow a grasping–picking–unloading action by the end-effector. The end-effector was analyzed by using a rigid kinetics simulation. A three-dimensional (3D) model was drawn by using the software Pro/Engineer and saved in X-T intermediate format [33]. These files were then imported into a rigid kinetics simulation model in ADAMS, and the kinetics of the structure as a whole was analyzed [34]. The consistency of motion between the bionic fingers and their ability to pick fruit were considered [35], and we examined whether the coordination between the fingers met the requirements for integrated harvesting action. The simulation software analyzed the mechanical movement, model structure, and mesh generation, and we used a kinetics simulation to analyze the move-

ment of the picking end-effector. The analysis of the picking action was used to select a smooth trajectory.

The mechanical analysis module of the modeling procedure was used to establish relations between the connected components. In the analysis of the rigid body kinetics, the hinge relation between the rigid bodies was determined mainly by a joint and spring command. In the contact relation, the surface of the tracking groove was selected as the target surface and the outer surface of the plug as the contact surface. Next, in the mechanical analysis module, we established the connection and contact relation between the components. The outer surface of the bolt was selected as the contact surface. Bolts and bearings were built by a joint connection mode. A general joint was selected between joints with rotation relations. This joint had all degrees of freedom or could move in the X, Y, and Z directions and in the direction of the axis of rotation. A fixed joint was set at the bottom of the support frame, which was used as a rack. The analysis of the rigid body kinetics defines a single rigid body as a particle, where a single particle is a unit. The results of the simulation of the end-effector's trajectory show the trajectories

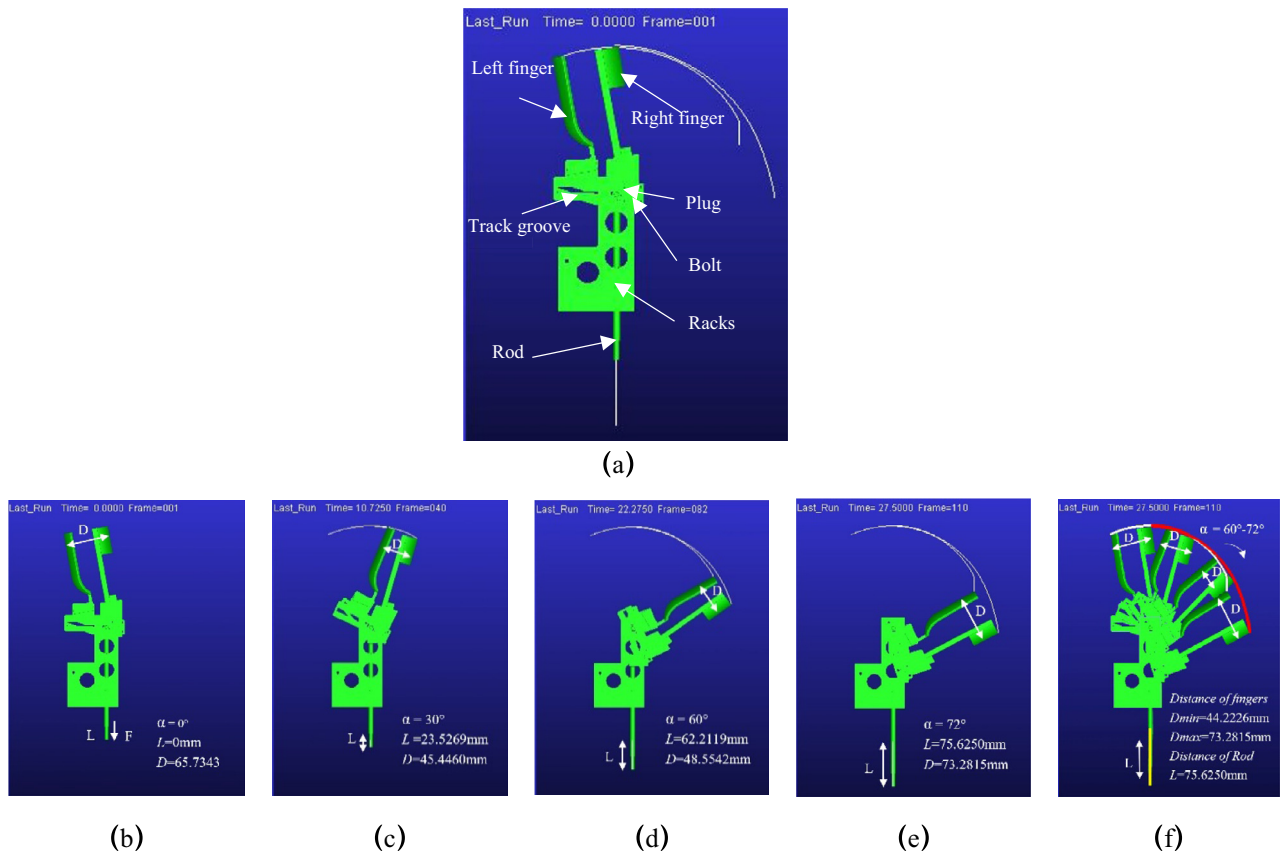


Fig. 6 – Simulated trajectory of end-effector in ADAMS. Step positions at different time points during motion. (a) The contact relations between components of the end-effector. The end-effector (b) opens its fingers, and (c) closes its fingers for grasping, (d) picking, and (e) unloading. (f) The overall process. The white line is the trajectory of the left finger; the red line is that of the right finger, and the yellow line is the trajectory of the rod. The white arrows indicate the distance between the fingers.

of the fingers and the rod. We chose the top of the medial finger of the end-effector (which was in contact with the fruit's surface) as the trajectory point. Fig. 6(a) shows the contact relations among components in the simulation of the end-effector.

The contact relations between the various parts of the end-effector, including the frictionless contact relation between the track's groove surface and the bolt, the joint contact relations, and the axial rotational degrees of freedom between the bolt and bearing, were established in the ADAMS model for trajectory analysis. When the velocity of the rod was 0.2 ms^{-1} and the pulling force was 15 N, the grasping, picking, and unloading movements of the end-effector met the predetermined requirements. The kinetic analysis revealed that the end-effector's locus of movement matched the trajectory of the bionic fingers in the picking process and that the end-effector was therefore suitable for its intended purpose. Fig. 6 shows the step simulation of the end-effector movement.

2.4. Manufacture and control of end-effector

The end-effector was designed for the growing conditions of clustered kiwifruit under a scaffolding cultivation. The design of the end-effector considered the width of the finger. The

shape of the bionic fingers was based on the parameters of the kiwifruit given in Table 1. The bionic fingers were fabricated by a 3D printer. The left finger was $125 \text{ mm} \times 56 \text{ mm}$, and the right finger was $125 \text{ mm} \times 75 \text{ mm}$, with both having a radius of curvature of 32.5 mm [33]. The fault-tolerant fingers were wider than the major axis of the kiwifruit and were designed to accommodate variations in the position of the center of the kiwifruit. The pendulum angles of the bionic fingers were determined by assuming that the track groove of one finger was horizontal.

A prototype of the end-effector was assembled from components that included a fiber sensor (Guangzhou Gelong Electronics Ltd., E20), a Hall-effect position sensor (Tianjin Yueer Xing Electronic Technology Ltd., YS44E), a pressure sensor (FSR 402 Pressure Sensor, ADC 0832 Modulation circuit chip; Interlink Electronics, United States), and a stepper motor (Japan Sawano Ltd., SW1720N10A). The main parts of the hardware of the control system consisted of a single-chip computer, a sensor, and a motor driver. We used the Keil development suite to write the computer program in C. The control system had two power supply modules. The control signal voltage for the sensor, single-chip computer, and motor driver was +5 V, and that for the stepper motor driver was +24 V. Fig. 7 shows the prototype control part of the hardware.

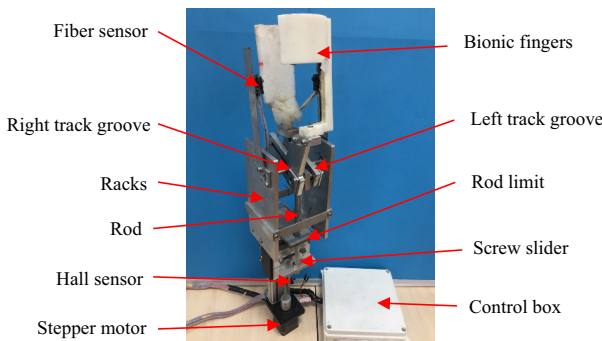


Fig. 7 – Prototype of end-effector consisting of a sensor, machinery, and control system. The stepper motor drives the screw slider. The rod moves upwards in the left and right track grooves, and the fingers start picking.

The working principle is as follows: First, the end-effector approaches a fruit, and the fiber sensor detects when the fingers have enveloped the fruit. Second, the motor initiates the downward movement of the pull rod in the specified stroke. The continuous compound action by the two fingers of grabbing–picking–unloading is guided by the reverse cam groove. Finally, as the end-effector picks the fruit, the motor forces an upward movement of the pull rod to reset the position of the end-effector. A processing flowchart for the end-effector is shown in Fig. 8.

2.5. Prototype of kiwifruit-harvesting robot

The prototype of the kiwifruit-harvesting robot had five components: the end-effector, a Cartesian coordinate manipula-

tor (CF3-3, Chong Feng Seiko Ltd., China), a programmable logic controller (Delta DVP-40EH) with a human-machine interface (Delta DOP B07S410), an electric vehicle, and a machine-vision device [Kinect sensor V2 and Dell laptop, Intel (R) Core (TM) i5-8250U CPU 1.60 GHz, 4 GB, NVIDIA GeForce MX150]. In addition, a light-emitting diode (LED) ensured constant illumination at night (CM-LED 1200HS, KEMA Co., Wuhan, China). The end-effector was assembled onto the experimental platform of the kiwifruit-picking robot. Figs. 9 and 10 represent schematic of the components of the harvesting robot system and photographs of parts of the system, respectively.

The machine-vision system of the harvesting robot recognized kiwifruit by using the Kinect sensor installed on the rack of the harvesting robot. When the harvesting robot was working, the Kinect sensor was responsible for information acquisition, and the computer was responsible for information processing. Fig. 11 shows an example of the recognition and location of kiwifruit in an RGB image. The Kinect sensor acquired color images from an RGB camera and depth images from an infrared camera and transmitted them to the computer. The computer applied a convolution neural network to detect the kiwifruit positions in the RGB image by using the Faster R-CNN method implemented in MATLAB (AlexNet), and extracted their coordinates. The Lidar and point cloud-processing module of MATLAB was used to generate point clusters. The depth map was combined with the RGB image to give the 3D coordinates of any point on the RGB image. Finally, the coordinates obtained by the convolutional neural network and recognition were mapped to the point cloud concentration to obtain the 3D coordinates of the kiwifruit. The horizontal (X and Y directions) and vertical (Z direction) coordinates of the tree picking point were calculated from a coordinate transformation of the kiwifruit.

3. Results

The kiwifruit-harvesting robot prototype was assembled for experimental testing in an orchard at the Meixian Kiwifruit Experimental Station of the Northwest Agriculture and Forestry University (Fig. 12). In experiments to test the practicability of the prototype, a Cartesian coordinate manipulator

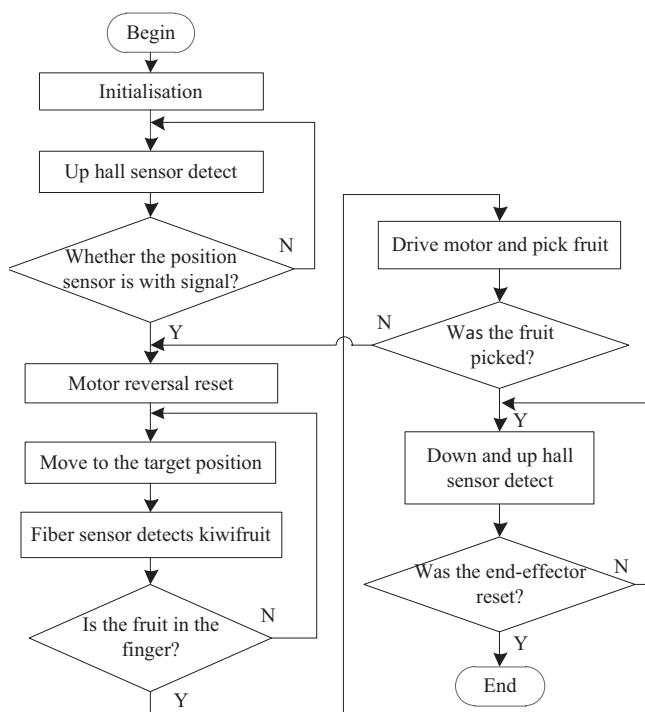


Fig. 8 – Flowchart for picking, showing the control process of the end-effector.

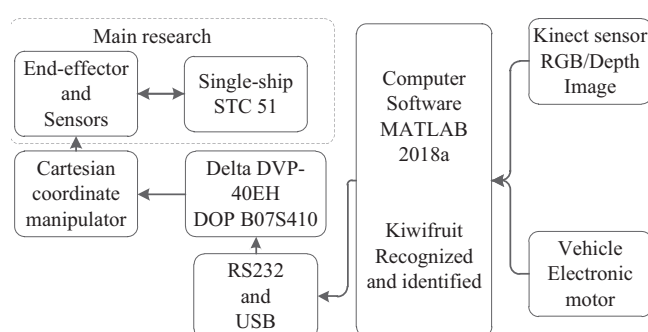


Fig. 9 – Main parts of the harvesting robot system: end-effector, Cartesian coordinate manipulator, machine vision device, vehicle, human-machine interface (HMI), and a control box with a programmable logic controller (PLC).

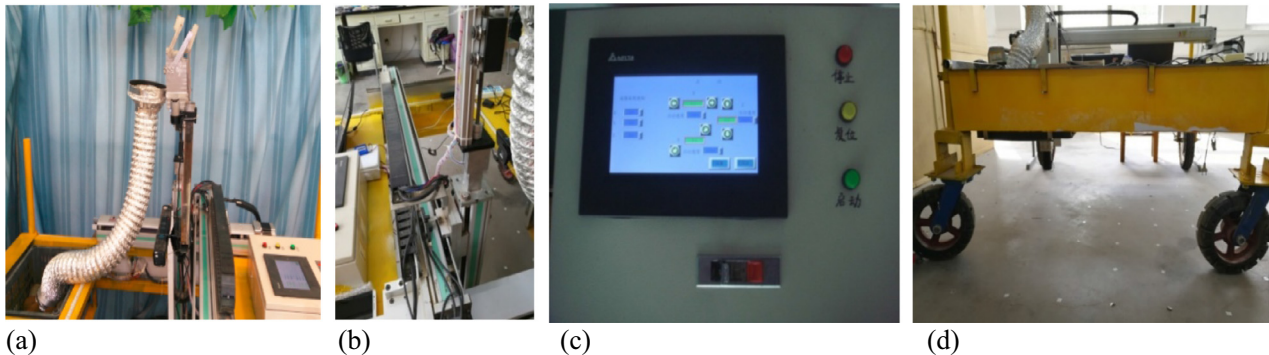


Fig. 10 – The kiwifruit harvesting robot system. (a) The kiwifruit harvesting robot, (b) the coordinate manipulator that can move in three dimensions, (c) the control box containing the entire control system for the harvesting robot, and (d) the electric vehicle with two universal wheels and two electric wheels.

moved the end-effector to the target fruit, and the end-effector then approached, grabbed, picked, and unloaded the fruit automatically.

3.1. Picking experiment

A field picking test was done in October 2018 in which 240 clustered fruits were harvested. The test lasted from 09:00 to 20:00 in three stages: 90 samples were collected from 09:00 to 11:00, 90 samples from 15:00 to 17:00, and 60 samples from 19:00 to 20:00 (with artificial lighting at night). The picking of a kiwifruit consisted of three steps: (1) The kiwifruit was grasped by the bionic fingers with gradually increasing clamping pressure, (2) when the sheer force was sufficiently strong, the fruit was detached from the stalk, and (3) the bionic fingers opened to release the picked fruit, which tumbled into the collection basket protected by the soft buffer material. This picking process is illustrated in Fig. 13, and typical picked kiwifruit are shown in Fig. 14.

Natural variations in the connection between kiwifruit and stem and between stem and tree meant that some picked kiwifruit retained their stems. Factors affecting the harvesting success rate include fruit maturity (the kiwifruit were harvested during the fruit season), length of the fruit stalk, clamp moment, bending angle and scope, and the presence of tree branches, scaffolding, and potholes in the ground (which can affect coordinate determination). Unsuccessful harvesting may be due to the separation of adjacent fruits, failure to grab the fruit properly, and the fingers slipping.

The success rate was calculated as the number of fruits successfully picked divided by the number of attempted picks. In the experiment, with 240 kiwifruit samples picked in total, the average success rate was 94.2%, as shown in Table 2. Dropping a kiwifruit may damage its peel, and 4.9% of kiwifruit picked in this experiment had damaged peels (Table 3). The average picking time was calculated for a cluster of fruit (2–6 fruit). The time started when the end-effector was in its initial position and ended when the entire cluster had been picked. This time was divided by the number of kiwifruit in the cluster. The average picking time was 4–5 s per fruit. This success rate is not acceptable because the machine is slower than a human. However, the percentage

of kiwifruit with damaged peels is less than with human pickers because fewer kiwifruit were dropped.

3.2. Data analysis

An analysis of the fruit-picking trajectory indicated that the centroid of vertical motion was 35 mm and the angle of rotation of the fruit was $70^\circ \pm 2^\circ$. The trajectory was parabolic, with the fruit and stalk forming an angle of $60^\circ\text{--}90^\circ$, which required minimum force for separation. The fingers continued to rotate to an open position, and the fruit was released.

3.3. Analysis of trajectory simulation

We provide a precise description of the simulation results in ADAMS, their interpretation, and the experimental conclusions that can be drawn. We simulated the trajectory of the fingers and the grasping-picking-unloading movement of the rod. The finger spacing was changed via the pull rod driving track slot. The relationship between finger spacing and distance traveled by the rod is shown in Fig. 15, and the parameters are given in Table 4. The fruit-picking trajectory shows the initial position of the fingers, and where they grasped, picked, and unloaded a kiwifruit, which eventually separated from the stem. Fig. 16 shows the displacement in different directions of the finger of the end-effector.

4. Discussion

The separation of the kiwifruit from the stalk was easiest to achieve when the long axis of the fruit and the stem's peduncle formed a 60° angle, as shown in Fig. 17. The minimum clamping force was 1.08 N, the minimum fruit-stem separation force was 1.38 N, and the average separation force was 3.68 N. The maximum pressure under compression reached 18.75 kPa, close to the theoretical value [5,30]. Compared with other end-effectors [5], the one used here integrates the grabbing, picking, and unloading operations by exploiting the trajectory model and the connecting rod linkages. Each picking movement took approximately 3 s, but unloading the fruit

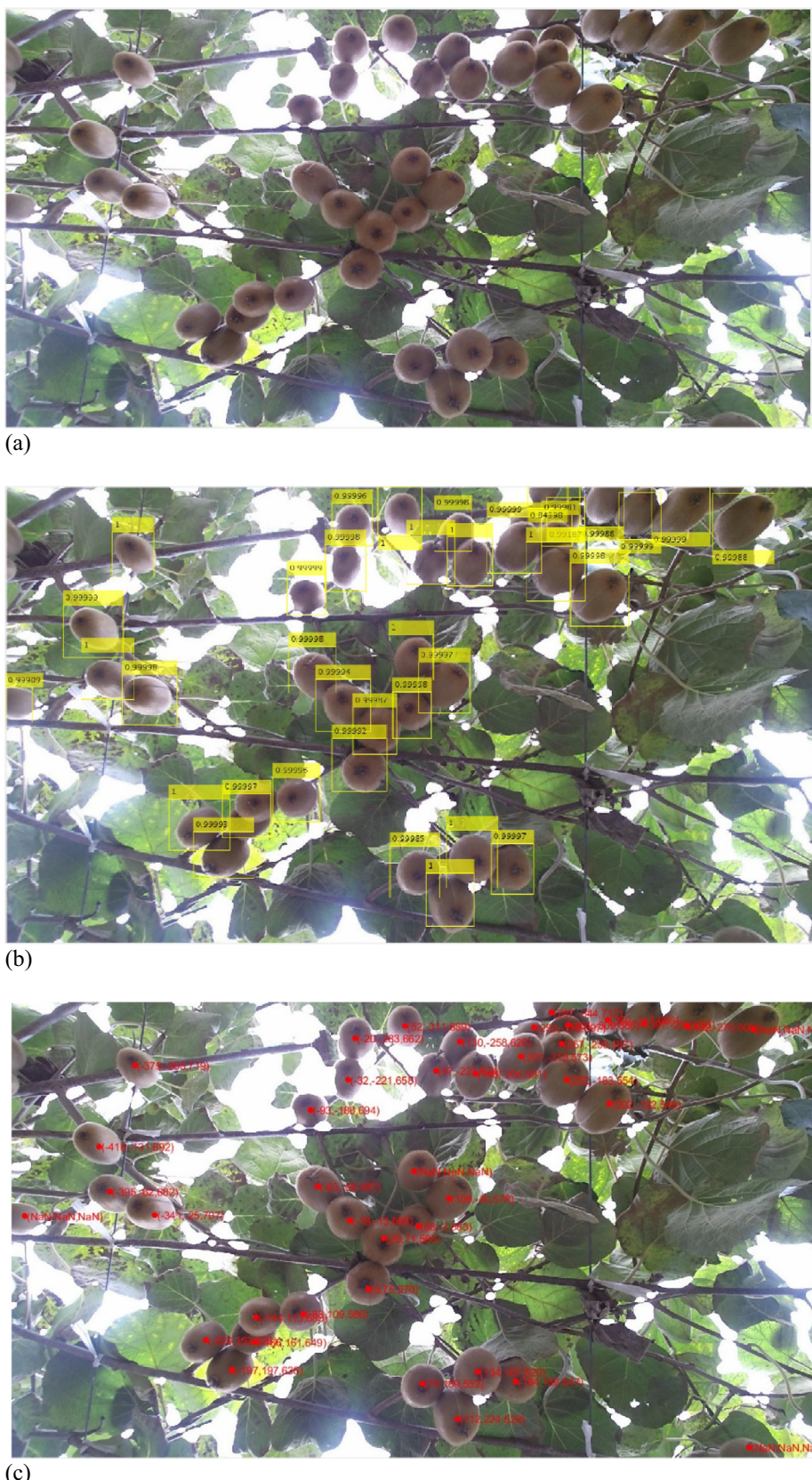


Fig. 11 – Kiwifruit recognition and location in an orchard. (a) RGB image of kiwifruit. (b) Kiwifruit recognized by AlexNet in MATLAB 2018a. (c) Coordinates of fruit (x, y, z).



Fig. 12 – Experimental kiwifruit-harvesting robot in the orchard with its integrated end-effector. Human-machine interface (HMI).

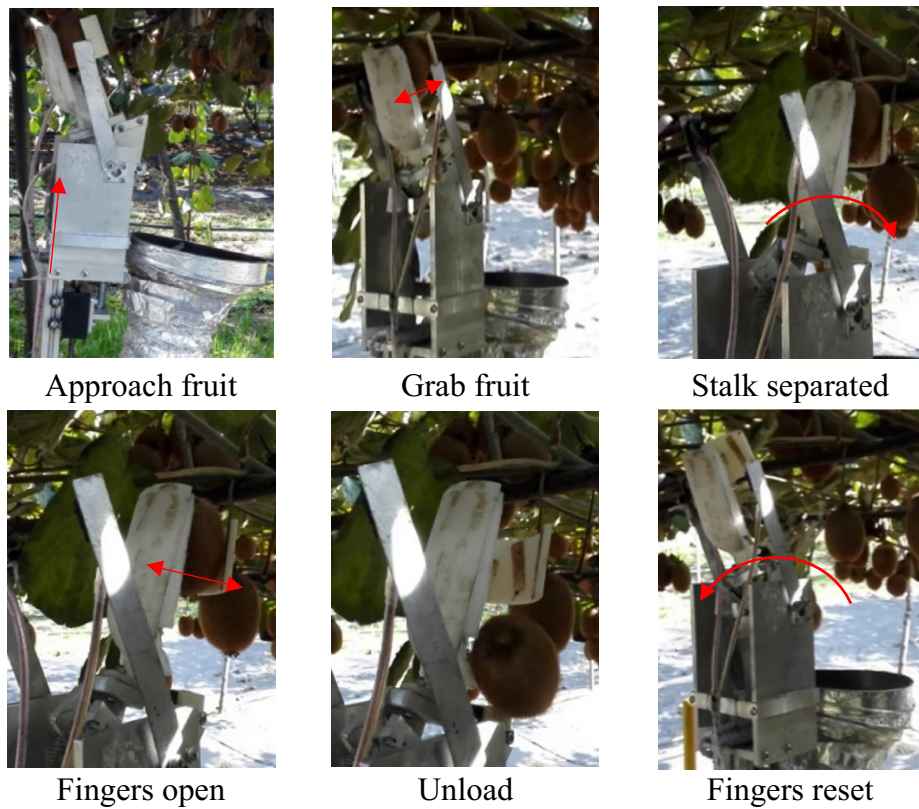


Fig. 13 – Harvesting of kiwifruit using the end-effector. Fruit-picking trajectory: as the end-effector fingers pull down, the kiwifruit and stalk eventually separate, and the fruit falls into the collection basket.

took no time. While the manipulator arm moved to the next working position, the end-effector was reset to its initial working position.

A comparative analysis shows that the picking accuracy of the end-effector was affected by offset in the positions of the fingers, assembly clearance error, fruit dropping, and the surface roughness of the fruit [12,19]. Crowding by adjacent fruit could cause difficulties in determining the coordinates, thereby preventing the end-effector from being correctly positioned for picking. To solve this problem, the width of the fin-

gers was optimized to have a 25 mm tolerance, allowing them to envelop kiwifruit of different sizes and shapes, even those with skewed growth. Conversely, if the end-effector attempted to pick a very small fruit, the fruit slipped from the fingers and was not picked (holding stage). This is because the separation force was too small for small fruit. To remedy this, a spring plate will be attached to the inside of the bionic fingers of the end-effector. The distance between the fingers of the spring plate should be suitable for grasping kiwifruit with a minor axis of 42.70–51.84 mm (Table 1). The clamping

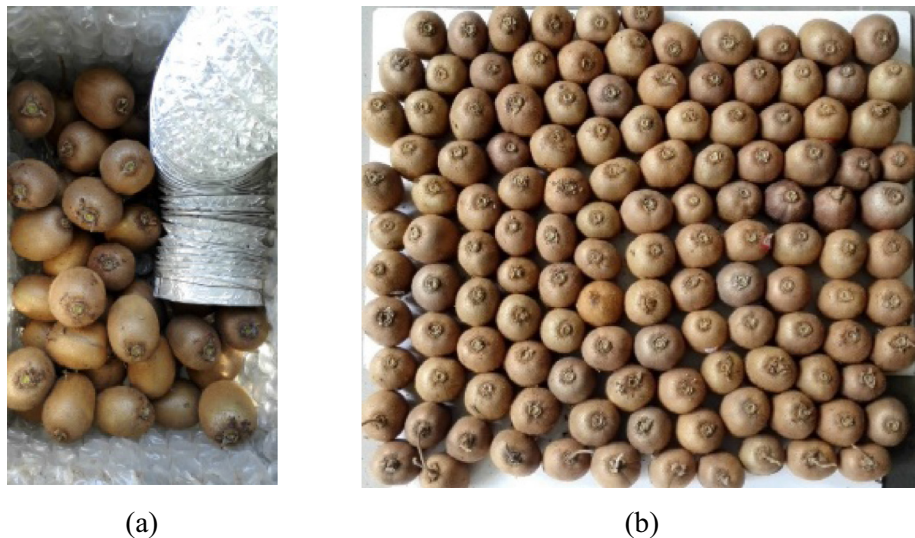


Fig. 14 – Fruits picked by the end-effector of the harvesting platform. (a) Kiwifruit falling into collection basket. (b) Some of the picked kiwifruit retain their stems.

Table 2 – Comparison of the success rates of kiwifruit samples at different picking times.

	09:00 to 11:00	15:00 to 17:00	19:00 to 20:00
Total attempted	90	90	60
Number successfully picked	86	82	58
Number of failures	4	8	2
Success rate	95.6%	91.1%	96.7%

Table 3 – Damage rate of picking.

	09:00 to 11:00	15:00 to 17:00	19:00 to 20:00
Total number picked	86	82	58
Number of kiwifruit with stem	3	4	6
Number of kiwifruit with peel damage	5	3	3
Damage rate	5.8%	3.7%	5.2%

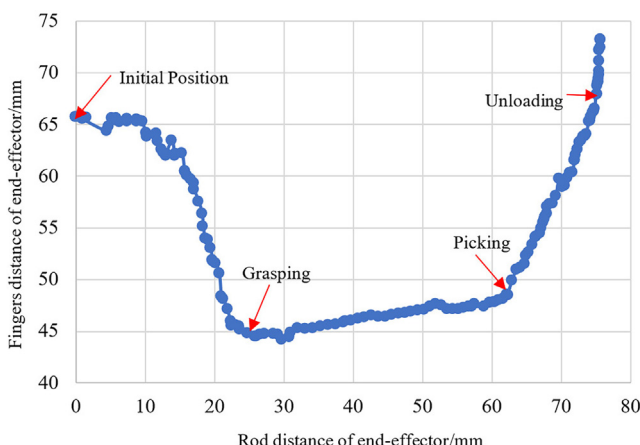


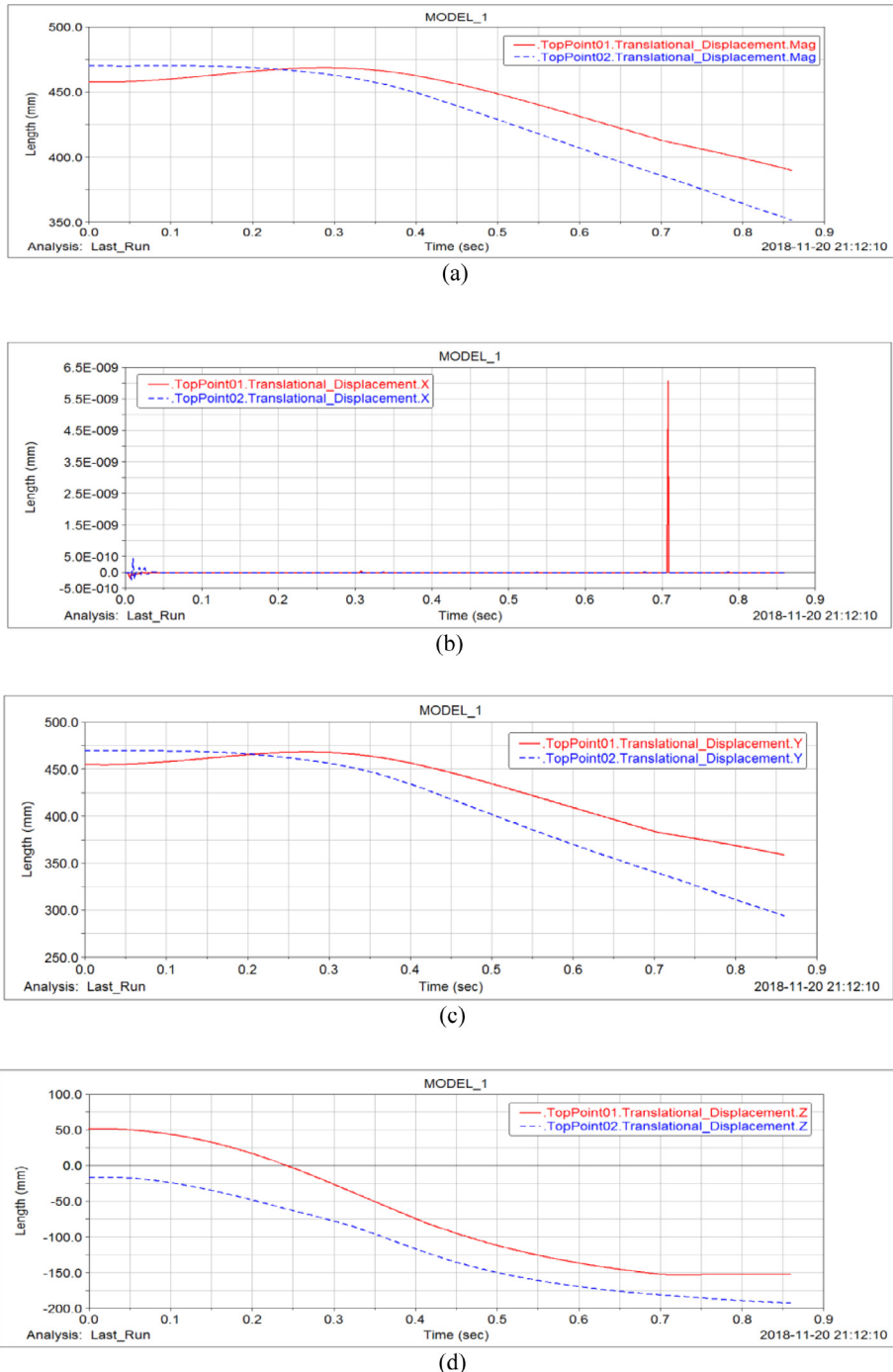
Fig. 15 – Relationship between spacing of the fingers and movement of the rod. The finger spacing is changed by the pull rod driving the track slot to simulate the movement of the two fingers of the end-effector in grasping-picking-unloading.

pressure of the finger can be adjusted by the spring so that the pressure reaches the threshold of the pressure sensor to prevent slippage when picking small fruit.

Fig. 18 shows the relationship between the actual distance from the Kinect sensor to the kiwifruit and the measured distance. The measurement was accurate for small distances, but if the kiwifruit was far from the Kinect sensor, the depth signal was weaker, and the contour of the kiwifruit was small compared with the distance to the target fruit. The distance error between the bottom of the kiwifruit (the calyx) and the sensor was small for distances in the range 0.5–1.0 m, which satisfies the requirement for a picking robot with an end-effector. According to the visual positions of 30 randomly selected fruit, the maximum error was 7.55 mm in the X direction and 15.3 mm in the Z direction. For these fruits, there were 28 successful fruit-stem separations carried out by the end-effector, showing that it can tolerate errors in the visual positioning system. The distribution of position errors is plotted in Fig. 19. Errors in the tree-picking point

Table 4 – Relation between rod distance and finger spacing.

Movement position	Rod distance (mm)	Finger spacing (mm)	Time (s)
Initial position	0	65.73	0.00
Grasping	23.53	45.45	0.39
Picking	62.21	48.55	0.81
Unloading	75.63	73.28	1.00

**Fig. 16 – Displacement of fingers of the end-effector. (a) The displacement along the compound direction of the finger of the end-effector. (b) X-direction displacement. (c) Y-direction displacement. (d) Z-direction displacement.**

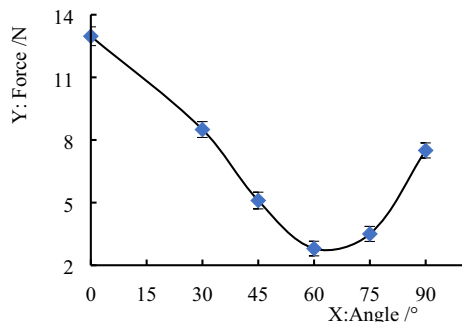


Fig. 17 – The force required to separate a kiwifruit from its stalk is least when the long axis of the fruit forms an angle of 60° with the stem's peduncle.

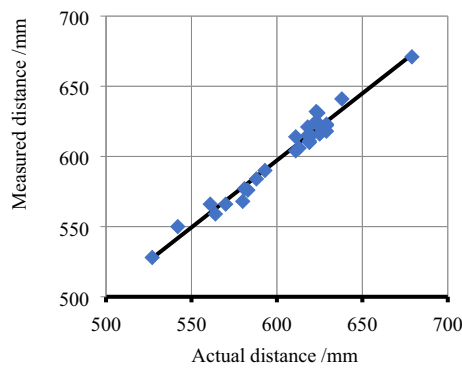


Fig. 18 – Relationship between actual distance and distance measured by the Kinect sensor. Error in the distance along the Z direction between the bottom of the kiwifruit (the calyx) and the sensor is small and meets the tolerance for a picking robot with an end-effector.

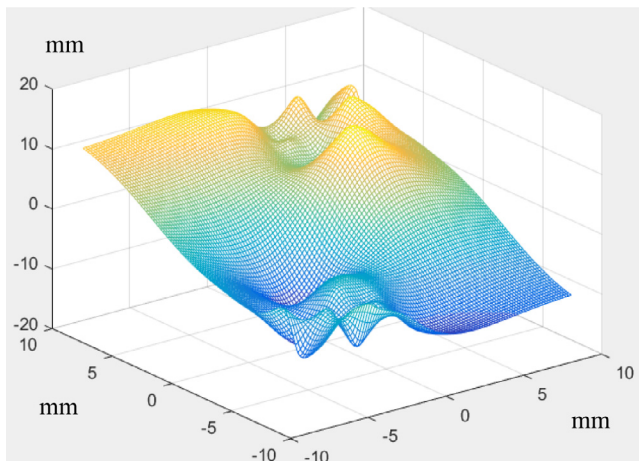


Fig. 19 – Distribution of position errors obtained from a statistical analysis of the centroids of 30 fruits as determined by the end-effector. Both the highest and the lowest positions are extreme errors that probably do not accurately represent the performance of the effector.

were calculated from the visual positioning error. The design of the end-effector should be tolerant of errors in visual positioning. Both the highest and the lowest positions were extreme errors that probably do not accurately represent the performance of the end-effector.

5. Conclusions and future research

This paper presents an end-effector designed and tested to pick kiwifruit grown in a scaffolding cultivation. The results show that the force required to separate a kiwifruit from its stem is minimal when the long axis of the fruit and the stem's peduncle form a 60° angle. These findings were exploited by the end-effector, which used bionic fingers to implement integrated picking and unloading of kiwifruit via a converse cam mechanism. This method considers the growth features and physical properties of the fruit. This end-effector approaches the fruit from below and grabs it with two fingers, which then bent the fruit downward to separate it from its stem. The mechanism of the end-effector is simple. The grabbing, picking, and unloading processes are integrated, with automatic picking and unloading performed using a connecting rod linkage following a trajectory model. Picking requires 4–5 s per kiwifruit on average and has a success rate of 94.2%. This study shows the potential of using a grabbing–picking–unloading end-effector for an automated kiwifruit-harvesting robot. However, the end-effector is too slow, so the prototype needs to be improved. The track slot error needs to be reduced so that the groove mechanism runs smoothly.

For the practical application and commercialization of the end-effector, future research needs to focus on the following three aspects: (1) Given the complex and diverse working environments encountered in fruit picking, real-time avoidance of trees and other obstacles is important for end-effectors. This requires the development of software and robust algorithms to improve the success rate and efficiency of the harvesting process. (2) The mechanical structure of the robot needs to be enhanced, for example by incorporating an adaptable articulated manipulator and end-effector to pick kiwifruit of different shapes and sizes. (3) Multi-target recognition and multi-manipulator coordination can be applied by the control system to improve the picking efficiency of the robot, thereby increasing its versatility, reducing overall cost, and promoting its commercialization.

We suggest that governments worldwide should introduce policies to promote the development of fruit-picking robots to reduce the labor costs associated with fruit picking.

Declaration of Competing Interest

The authors have no conflict of interest to declare.

Acknowledgments

This research was conducted in the College of Mechanical and Electronic Engineering, Northwest A&F University, and was supported by research grants from the General Program

of the National Natural Science Foundation of China (61175099). The authors have no financial interests to declare.

Appendix A. Supplementary material

Supplementary data to this article can be found online at <https://doi.org/10.1016/j.inpa.2019.05.004>.

REFERENCES

- [1] FAOSTAT. UN Food and Agriculture Organization. Kiwifruit production in 2016. UN Food and Agriculture Organization, Statistics Division; 2016.
- [2] Garcia-Quiroga M, Nunes-Damaceno M, Gomez-Lopez M, et al. Kiwifruit in syrup: consumer acceptance, purchase intention and influence of processing and storage time on physicochemical and sensory characteristics. *Food Bioprocess Tech* 2015;8(11):2268–78.
- [3] Shamshiri RR, Weltzien C, Hameed IA, et al. Research and development in agricultural robotics: a perspective of digital farming. *Int J Agr Biol Eng* 2018;11(4):1–14.
- [4] Hayashi S, Shigematsu K, Yamamoto S, et al. Evaluation of a strawberry-harvesting robot in a field test. *Biosyst Eng* 2010;105(2):160–71.
- [5] Fu LS, Zhang FN, Yoshinori G, et al. Development and experiment of end-effector for kiwifruit harvesting robot. *Trans Chin Soc Agric Mach* 2015;46(3):1–8.
- [6] Bac CW, van Henten EJ, Hemming J, et al. Harvesting robots for high-value crops: state-of-the-art review and challenges ahead. *J field robot* 2014;31(6):888–911.
- [7] Monta M, Kondo N, Ting KC. End-effectors for tomato harvesting robot. *Artif Intell Rev* 1998;12(1–3):11–25.
- [8] Kondo N, Monta M, Fujiura T. Basic constitution of a robot for agricultural use. *Adv Robot* 1996;10(4):339–53.
- [9] Zhao YS, Gong L, Huang YX, et al. Robust tomato recognition for robotic harvesting using feature images fusion. *Sensors* 2016;16(2):173–84.
- [10] Kondo N, Nishitsuji Y, Ling PP, et al. Visual feedback guided robotic cherry tomato harvesting. *Trans ASABE* 1996;39(6):2331–8.
- [11] Liu JZ, Li PP, Mao HP. Mechanical and kinematic modeling of assistant vacuum sucking and pulling operation of tomato fruits in robotic harvesting. *Trans ASABE* 2015;58(3):539–50.
- [12] Van Henten EJ, Hemming J, Van Tuijl BAJ, et al. An autonomous robot for harvesting cucumbers in greenhouses. *Auton Robot* 2002;13(3):241–58.
- [13] Ota T, Bontsema J, Hayashi S, et al. Development of a cucumber leaf picking device for greenhouse production. *Biosyst Eng* 2007;98(4):381–90.
- [14] Zhao DA, Lv JD, Ji W, et al. Design and control of an apple harvesting robot. *Biosyst Eng* 2011;110(2):112–22.
- [15] Li GL, Ji CY, Gu BX, et al. Kinematics analysis and experiment of apple harvesting robot manipulator with multiple end-effectors. *Trans Chin Soc Agric Mach* 2016;47(12). pp. 14–21 and 29.
- [16] Silwal A, Davidson JR, Karkee M, et al. Design, integration, and field evaluation of a robotic apple harvester. *J Field Robot* 2017;34(6):1140–59.
- [17] Davidson JR, Hohimer CJ, Mo C, et al. Dual robot coordination for apple harvesting. *ASABE Annual International Meeting*, Spokane, WA, United States; 2017.
- [18] Cui YJ, Gejima Y, Kobayashi T, et al. Study on cartesian-type strawberry-harvesting robot. *Sensor Lett* 2013;11(6–7):1223–8.
- [19] Lehnert C, English A, McCool C, et al. Autonomous sweet pepper harvesting for protected cropping systems. *IEEE RA-L* 2017;2(2):872–9.
- [20] Bac CW, Hemming J, van Tuijl BAJ, et al. performance evaluation of a harvesting robot for sweet pepper. *J Field Robot* 2017;34(6):1123–39.
- [21] Feng QC, Zou W, Fan PF, et al. Design and test of robotic harvesting system for cherry tomato. *Int J Agr Biol Eng* 2018;11(1):96–100.
- [22] Chen J, Wang H, Jiang H, et al. Design of end-effector for kiwifruit harvesting robot. *Trans Chin Soc Agric Mach* 2012;43(10). pp. 151–154+199.
- [23] Li J, Karkee M, Zhang Q, et al. Characterizing apple picking patterns for robotic harvesting. *Comput Electron Agr* 2016;127:633–40.
- [24] Shi YG, Zhu KJ, Zhai SH, et al. Design of an apple-picking end effector. *STROJ VESTN-J Mech E* 2018;64(4):216–24.
- [25] Mehta SS, Burks TF. Vision-based control of robotic manipulator for citrus harvesting. *Comput Electron Agr* 2014;102:146–58.
- [26] Mehta SS, MacKunis W, Burks TF. Robust visual servo control in the presence of fruit motion for robotic citrus harvesting. *Comput Electron Agr* 2016;123:362–75.
- [27] You K, Burks T. Development of a robotic fruit picking end effector and an adaptable controller. *ASABE Annual International Meeting*, Orlando, FL, United States; 2016.
- [28] Luo LF, Tang YC, Zou XJ, et al. Vision-based extraction of spatial information in grape clusters for harvesting robots. *Biosyst Eng* 2016;151:90–104.
- [29] Mu LT, Liu HZ, Cui YJ, et al. Mechanized technologies for scaffolding cultivation in the kiwifruit industry: a review. *Inform Process Agric* 2018;5(4):401–10.
- [30] Ji W, Qian ZJ, Xu B, et al. Grasping damage analysis of apple by end-effector in harvesting robot. *J Food Process Eng* 2017;40(6):1–8.
- [31] Scarfe AJ. Development of an autonomous kiwifruit harvester: a thesis presented in partial fulfilment of the requirements for the degree of Doctor of Philosophy in Industrial Automation at Massey University, Manawatu, New Zealand; 2012.
- [32] Scarfe AJ, Flemmer RC, Bakker HH, et al. Development of An Autonomous Kiwifruit Picking Robot. In: *Proceedings of the Fourth International Conference on Autonomous Robots and Agents*. p. 639–43.
- [33] Mu LT, Liu YD, Cui YJ, et al. Design of End-effector for Kiwifruit Harvesting Robot Experiment. Spokane, WA, United states: *ASABE Annual International Meeting*; 2017.
- [34] Carabin G, Gasparetto A, Mazzetto F, et al. Design, implementation and validation of a stability model for articulated autonomous robotic systems. *Robot Auton Syst* 2016;83:158–68.
- [35] Zhao DY, Li SY, Zhu QM. Adaptive synchronised tracking control for multiple robotic manipulators with uncertain kinematics and kinetics. *Int J Syst Sci* 2016;47(4):791–804.